Complex Modes in Shielded Suspended Coupled Microstrip Lines

JEN-TSAI KUO, STUDENT MEMBER, IEEE, AND CHING-KUANG C. TZUANG, MEMBER, IEEE

Abstract—**The existence of complex modes in electrically shielded suspended coupled microstrip lines has been studied extensively, and the results are presented. A rigorous full-wave spectral-domain approach (SDA) with a newly proposed and tested set of basis functions can efficiently and accurately determine the propagation characteristics of the dominant, higher order, and complex modes for planar or quasi-planar transmission lines. These basis functions are validated by comparing the convergence study of field solutions with those obtained by various sets of preconditioned bases and by the unconditioned subdomain ones. Excellent agreement is obtained for the propagation constants and the normalized complex longitudinal and transverse current distributions on conducting strips for the strongly coupled microstrip lines. This suggests that the proposed set of basis functions can be a viable candidate for the SDA in analyses of planar or quasi-planar transmission lines.**

Under all the particular case studies of this paper, it is shown that the complex modes may exist in all the shielded suspended coupled microstrip lines, even when the substrate dielectric constant is low. Theoretical results for the fundamental, higher order, evanescent, and complex modes are presented for suspended coupled microstrip lines.

1. INTRODUCTION

PLANAR AND quasi-planar transmission lines are the most commonly used waveguides in microwave and millimeter-wave integrated circuits [1], [2]. Various applications such as impedance matching, filter, and coupler designs may inevitably introduce discontinuities into the passive circuits. Therefore the characterization of planar or quasi-planar transmission line discontinuities becomes an important task for the computer-aided design (CAD) of microwave and millimeter-wave integrated circuits [3]. For electrically shielded planar and quasi-planar transmission lines, many authors have reported that the fundamental, higher order, evanescent and complex modes may coexist [4]–[7]. As Omar and Schünemann reported in their work of finline analysis [4], complex modes and backward-wave modes may exist in any planar guiding structure with closed boundaries. Later the inhomogeneously and anisotropically filled waveguides [5] and the symmetric microstrip line [6], [7] were also found to support complex modes. Overlooking either one or both of a pair of complex modes in the waveguide discontinuity analysis may lead to an irregularity of circuit parameters in the entire frequency spectrum of interest [8].

So far two methods for obtaining the solutions of the complex modes for microstrip and slotlines (or finlines) have been reported. The singular integral equation (SIE) technique has been efficiently applied to analyze a symmetric finline [4] and a microstrip line [6]. In the literature [7], a discrete space-domain formulation has been used to calculate various modes for a symmetric microstrip line in closed structure.

Notice that all the reported solutions of the complex modes are for symmetric transmission lines. Besides the SIE and the discrete space-domain approach, the spectral-domain approach (SDA) is the most widely used method in analyzing millimeter-wave planar or quasi-planar transmission lines for the dominant and the first few higher order modes [4]. This paper extends the SDA to analyze the possible existence of complex modes in symmetric or asymmetric planar or quasi-planar transmission lines embedded in a layered dielectric medium. Should both longitudinal and transverse current distributions on each conducting strip be correctly obtained for any type of modal solution, the field solutions would be exact. One of the objectives of this paper is to obtain currents that are as close to being true as possible for any modal solution of general printed circuit lines. To achieve this, a newly proposed set of basis functions satisfying the criteria reported by Jansen [9] is derived from a two-dimensional electrostatic wedge problem.

Subsection II-A briefly describes the basic features of the SDA, and subsection II-B lists the proposed set of basis functions with detailed discussions. Subsection II-C qualitatively compares the numerical efficiency of the proposed bases with various types of preconditioned bases, namely 1) the sinusoidal type [10], [11], i.e., Fourier sine and cosine series divided by a term that corresponds to the edge singularity of an infinitely thin metal strip, and 2) the Chebyshev type [12], i.e., Chebyshev functions of the first and second kinds modified by the edge condition. These two sets of basis functions will be designated as S (sinusoidal) type and C (Chebyshev) type herein.

To test the accuracy of results obtained by using the proposed bases, subsection III-A performs a comparative convergence study of the complex modes obtained by

Manuscript received March 31, 1989; revised April 17, 1990. This work was supported in part by the National Science Council under NSC79-0404-E009-29.

The authors are with the Institute of Communication Engineering and MIST (Microelectronics and Information Science and Technology Research Center), National Chiao Tung University, 75 Po Ai Street, Hsinchu, Taiwan, Republic of China.

IEEE Log Number 9036769.

0018-9480/90/0900-1278$01.00 ©1990 IEEE

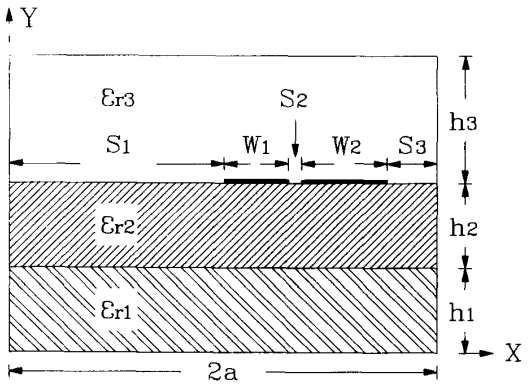

Fig. 1. Cross-sectional view of the asymmetric coupled microstrip lines embedded in a layered dielectric medium.

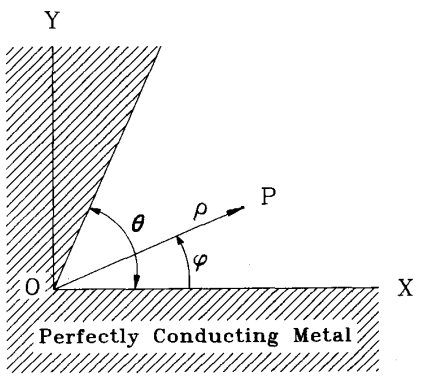

Fig. 2. A two-dimensional corner defined by an intersection of two conducting planes.

various types of basis functions for asymmetric strongly coupled microstrip lines. Because the entire-domain (or global) basis functions are preconditioned, it is necessary to test whether the results obtained by the proposed bases are the same as those obtained by the unconditioned ones, namely, the discretized or subdomain bases [13] (see also Section III). The subdomain bases are believed to be capable of representing true complex current distributions of single or coupled microstrip lines if each metal strip is partitioned into an adequate number of subsections. Subsection III-B compares the capability of representing true complex current distributions on the printed lines for various types of preconditioned bases and unconditioned subdomain bases. Subsection III-C presents the theoretical fundamental, higher order, evanescent, and complex modes of suspended coupled microstrip lines with different dielectric substrates.

II. Formulation

A. Spectral-Domain Approach

The SDA has been widely accepted for analyzing transmission lines, regardless of whether they are open or closed structures [14]. When analyzing the coupled microstrip lines embedded in a layered dielectric medium as shown in Fig. 1, the SDA is even more attractive if the concept of the immittance approach is invoked [15]. Conceptually the immittance approach, which combines network and field theories, provides much more physical insight than other techniques developed for microstrip and slotline analyses. For the structural geometry shown in Fig. 1, the SDA starts with the Fourier transform defined as follows:

$$F(\Psi(x,y)) = \int_{-\infty}^{\infty} \Psi(x,y)\cdot e^{j\alpha x}\,dx = \tilde{\Psi}(\alpha,y). \quad (1)$$

By the immittance approach [15], the dyadic Green's function $\tilde{Z}$ can be derived as

$$\begin{bmatrix} \tilde{Z}_{zz}(\gamma) & \tilde{Z}_{zx}(\gamma) \\ \tilde{Z}_{xz}(\gamma) & \tilde{Z}_{xx}(\gamma) \end{bmatrix} \cdot \begin{bmatrix} \tilde{J}_z \\ \tilde{J}_x \end{bmatrix} = \begin{bmatrix} \tilde{E}_z \\ \tilde{E}_x \end{bmatrix} \quad (2)$$

where γ is the propagation constant to be determined and $\exp(j\omega t - \gamma z)$ is assumed.

Next, the Galerkin procedure is applied to (2). The unknown surface current densities on each conducting strip are expanded by a complete set of basis functions. After matching the final boundary conditions imposed on the metal–dielectric interface, e.g., $y = h_1 + h_2$ in Fig. 1, a nonstandard eigenvalue problem can be formulated, namely

$$\det\left[G_{p\times p}(\gamma)\right] = 0. \quad (3)$$

The propagation constants (γ's) are the roots of (3). These roots may stand for the fundamental, higher order, evanescent, or complex modes for the coupled microstrip lines. The integer subscript p stands for the order of the square matrix $\boldsymbol{G}$.

B. The Proposed Set of Basis Functions and Its Derivation

Motivated to obtain very accurate modal solutions, including the possible existence of complex modes, we seek to develop an alternative set of basis functions. Jansen [9] listed six criteria for obtaining basis functions used in the SDA, namely 1) edge condition, 2) twice continuous differentiability, 3) completeness, 4) integral relationship between longitudinal and transverse currents of a microstrip line, 5) ability to represent nearly true modal current distributions, and 6) capability of being Fourier transformed. Now consider the two-dimensional electrostatic wedge problem shown in Fig. 2, in which the complete solution for the surface charge distribution at point $P|_{\varphi=0}$ can be expressed as [16]

$$\sigma(\rho) = \sum_{n=1}^{\infty} a_n \rho^{(n\pi/\theta)-1} \quad (4)$$

where ρ is the distance measured from the corner, and the a_n's are constants. For the infinitely thin microstrip lines shown in Fig. 1, $\theta = 2\pi$. Let us consider the proposed basis functions for the current distributions on strip 1 of width W_1 in Fig. 1 (the derivation of those for the currents on strip 2 is identical). Since the dielectric substrates are nonmagnetic, the longitudinal current $J_z(x)$ is

proportional to the charge distribution $\sigma(x)$ under quasi-TEM conditions [17]. Letting the normalizing variable $u_1 = 2/(X - S_1 - W_1/2)W_1$ and subsequently $\rho^{n/2-1} = (W_1/2)^{n/2-1}\cdot(1 \pm u_1)^{n/2-1}$ for $n = 1,2,\cdots$, we obtain $J_{z11}(u_1)$ corresponding to the edge at $u_1 = -1$ as

$$J_{z11}(u_1) = \sum_{n=1}^{\infty} b_{1n}(1+u_1)^{n/2-1} \tag{5}$$

and $J_{z12}(u_1)$ corresponding to the edge at $u_1 = 1$ as

$$J_{z12}(u_1) = \sum_{n=1}^{\infty} b_{2n}(1-u_1)^{n/2-1}. \tag{6}$$

In (5) and (6), the b_{1n}'s and b_{2n}'s are constants and $-1 < u_1 < 1$. The longitudinal current on strip 1, $J_{z1}(u_1)$, is the sum of $J_{z11}(u_1)$ and $J_{z12}(u_1)$:

$$\begin{aligned} J_{z1}(u_1) &= J_{z11}(u_1) + J_{z12}(u_1) \\ &= \sum_{m=1}^{2}\sum_{n=1}^{N_b} c_{1mn} j_{z1mn}(u_1). \end{aligned} \tag{7}$$

Notice that $J_{z11}(u_1)$ ($J_{z12}(u_1)$) is obtained by extending (4) at $u_1 = -1$ (+1). If $J_{z1}(u_1)$ is expected to depend only on $J_{z11}(u_1)$ ($J_{z12}(u_1)$) at $u_1 = -1$ (+1), $J_{z12}(u_1)$ ($J_{z11}(u_1)$) is to be forced to zero at $u_1 = -1$ (+1). One possible way of doing this is to adopt

$$\begin{aligned} j_{z1mn}(u_1) &= (1 \pm u_1)^{n/2-1} - \sqrt{2}(1 \pm u_1)^{n/2-1/2} \\ &\quad + \tfrac{1}{2}(1 \pm u_1)^{n/2} \end{aligned} \tag{8}$$

where plus is for $m = 1$, minus is for $m = 2$, and n is the order of the basis functions. In (7), N_b is the number of basis functions (j_{z1mn}) used in the SDA for the expansion of J_{z11} or J_{z12}. Notice that the edge condition of an infinitely thin strip is guaranteed by the asymptotic behavior of $J_{z1m}(u_1)$ at $u_1 = -1$ and 1 for $m = 1$ and 2, respectively. For example, as u_1 approaches -1, $j_{z111}(u_1)$ prevails and the asymptotic behavior $\delta^{-1/2}$ is guaranteed. On the strip away from the edges the longitudinal current distribution is then modeled by (7) and (8). Notice also that criterion 3 is satisfied by (7) and (8). It is obvious that the bases in (8) satisfy criterion 2.

By integrating the following continuity equation imposed on the metal strip as is done in [17],

$$\frac{\partial}{\partial x}(J_x(x)e^{-\gamma z}) + \frac{\partial}{\partial z}(J_z(x)e^{-\gamma z}) = -jw\sigma(x)e^{-\gamma z} \tag{9}$$

where $\sigma(x)$ has been defined in (4), we obtain

$$\begin{aligned} J_{x1}(u_1) &= J_{x11}(u_1) + J_{x12}(u_1) \\ &= \sum_{m=1}^{2}\sum_{n=1}^{N_b} d_{1mn} j_{x1mn}(u_1), \end{aligned} \tag{10}$$

and

$$\begin{aligned} j_{x1mn}(u_1) &= (1 \pm u_1)^{n/2} - \sqrt{2}(1 \pm u_1)^{n/2+1/2} \\ &\quad + \tfrac{1}{2}(1 \pm u_1)^{n/2+1} \end{aligned} \tag{11}$$

where the plus and the minus correspond to the subscript $m = 1$ and 2, respectively. Notice that $J_{x1}(u_1)$ vanishes at the rate of $\delta^{1/2}$ at $u_1 = -1$ and $u_1 = 1$. In addition, $j_{x11n}(1) = 0$ and $j_{x12n}(-1) = 0$ for all $n \geq 1$. By doing so, $J_{x11}(u_1)$ and $J_{x12}(u_1)$ have no influence on the transverse current distribution at the edges $u_1 = 1$ and $u_1 = -1$, respectively. Although there are many possible ways of doing this, (7) and (8) and (10) and (11) are found to be capable of modeling true current distributions.

When $n = 1$ and 2, the Fourier transforms of $(1+u_1)^{n/2-1}$ can be readily derived, and the results are

$$F\left[(1+u_1)^{-1/2}\right] = \frac{e^{-j\kappa}}{\sqrt{\kappa}} \cdot \frac{W_1}{2} \cdot \left[\mathcal{F}_c(2\kappa) + j\mathcal{F}_s(2\kappa)\right] \cdot e^{j\alpha x_c} \tag{12}$$

$$F\left[(1+u_1)^{0}\right] = \frac{1}{\kappa} \cdot W_1 \cdot \sin(\kappa) \cdot e^{j\alpha x_c} \tag{13}$$

where $\kappa = (\alpha W_1)/2$, $x_c = S_1 + \frac{1}{2}W_1$, and the Fourier transform variable $\alpha \geq 0$. $\mathcal{F}_c$ and $\mathcal{F}_s$ are respectively the Frensel cosine and sine integrals, defined by

$$\mathcal{F}_c(\xi) + j\mathcal{F}_s(\xi) = \int_0^{\xi} u^{-1/2} \cdot e^{ju}\, du. \tag{14}$$

By definition and by integrating by parts, $F[(1+u_1)^{n/2-1}]$ with $n \geq 3$ can be expressed as

$$\begin{aligned} F\left[(1+u_1)^{n/2-1}\right] = \frac{-j}{2\kappa}\Bigg\{ & 2^{n/2} \cdot e^{j\kappa} \cdot \frac{W_1}{2} \cdot e^{j\alpha x_c} \\ & - (n-2) \cdot F\left[(1+u_1)^{n/2-2}\right]\Bigg\}. \end{aligned} \tag{15}$$

Since $F[\Psi(-x)] = F^*[\Psi(x)]$ for any real function $\Psi(x)$, where the asterisk denotes the complex conjugate, the Fourier transform of $(1-u_1)^{n/2-1}$ can be readily obtained from that of $(1+u_1)^{n/2-1}$. The numerical evaluations of $\mathcal{F}_c$ and $\mathcal{F}_s$ can be found in [18]. Thus criterion 6 is satisfied. Now, only criterion 5 has not been addressed.

It is obvious that the basis functions in (8) and (11) are well suited to determine the current distributions on the asymmetric coupled microstrip lines in Fig. 1. Even in the case of a symmetric structure, e.g. a symmetric microstrip line, they automatically result in both even and odd modes of solutions.

C. Other Bases Commonly Used for Analyzing Asymmetric Structures by the SDA or Space-Domain Technique

Jansen [10] chose a complete set of basis functions satisfying the edge condition term by term to compute the characteristics of both shielded and open planar microwave and millimeter-wave transmission lines. Later, Schmidt *et al.* [11] used only two expansion terms of this set of basis functions to obtain both the propagation constant and the characteristic impedance with 0.5% accuracy for an arbitrarily located unilateral finline. Kobayashi *et al.* formulated closed-form expressions to approximate the unknown longitudinal and transverse current distributions on microstrip line [19] and coupled microstrip lines [20]. Both sets of closed-form expressions

have resulted in accurate dominant-mode solutions when they are employed in the SDA. However, the mathematical expressions of the basis functions for the coupled microstrip lines are complicated [20]. Recently, Faché and De Zutter [13], [21] analyzed single and coupled microstrip lines in the space domain using the method of moments to discretize each current component. Tripathi and Lee [12] used Chebyshev polynomials of the first and second kinds modified by the edge condition to compute the dispersive characteristics of multiple coupled line structures in an inhomogeneous medium.

One of the most advantageous features of the SDA is the fact that the preconditioned basis functions do not have to be very accurate to obtain a moderately accurate propagation constant for practical applications [19]. An insufficient number of basis functions and inaccurate bases, however, will result in poor SDA solutions [19], [20]. This is due to the fact that criterion 5 in subsection II-B is violated.

To verify the fact that the proposed set of bases is capable of modeling true currents, i.e., criterion 5, we incorporate the SDA basis functions employed in [10]–[12] into the analysis of asymmetric coupled microstrip lines for comparative study. The Fourier transforms for these sets of basis functions are listed here for reference.

1) Sinusoidal (S) Type [10],[11]:

$$\tilde{J}_{zn}(\alpha) = \frac{\pi}{2}\cdot W\cdot\left[B_0(\alpha W + p_n)\cdot e^{jp_n} + B_0(\alpha W - p_n)\cdot e^{-jp_n}\right] \quad (16)$$

$$\tilde{J}_{xn}(\alpha) = -j\frac{\pi}{2}\cdot W\cdot\left[B_0(\alpha W + p_n)\cdot e^{jp_n} - B_0(\alpha W - p_n)\cdot e^{-jp_n}\right] \quad (17)$$

where $p_n = (n/2)\pi$.

2) Chebyshev (C) Type [12]:

$$\tilde{J}_{zn}(\alpha) = (j)^n\cdot\pi\cdot W\cdot B_n(\alpha W) \quad (18)$$

$$\tilde{J}_{xn}(\alpha) = (j)^n\cdot\pi\cdot W\cdot(n+1)\cdot B_{n+1}(\alpha W)/(\alpha W). \quad (19)$$

In (16) through (19), the center of the strip is located at $x = 0$. B_n is the nth-order Bessel function of the first kind, $n = 0,1,2,\cdots$, and W is the half-width of the strip.

To compare the numerical efficiencies of the three sets of global or preconditioned bases, we must compare the CPU times used for setting up the determinantal matrix $\boldsymbol{G}$ in (3). For the proposed bases, a) $F[(1+u_1)^{n/2-1}]$, for $n \geqslant 3$, can be obtained by the application of recursive formula (15); b) $\tilde{j}_{x1mn}(\alpha) = \tilde{j}_{z1mp}(\alpha)$, $p = n+2$ for $m = 1$ or 2, ((8) and (11)); and c) $\tilde{j}_{z12n}(\alpha)$ and $\tilde{j}_{x12n}(\alpha)$ are the complex conjugates of $\tilde{j}_{z11n}(\alpha)$ and $\tilde{j}_{x11n}(\alpha)$, respectively, for $n = 1,2,\cdots,N_b$ (subsection II-B). Therefore the most time-consuming part is the evaluation of Fresnel integrals. The computations of $\tilde{j}_{z1mn}(\alpha)$ and $\tilde{j}_{x1mn}(\alpha)$ invoke simple algebraic computations on the stored data. Our experiences show that the CPU time of the SDA program using bases of the S type is nearly 10% more than that using bases of the C type or the bases proposed for implementing a determinantal matrix of size 32×32.

III. Results

The legitimacy of the proposed bases will be tested against the existing ones, namely, the preconditioned S and C types and the unconditioned subdomain bases. We choose a pair of asymmetric strongly coupled microstrip lines (Fig. 1) with aspect ratios of $S_1:W_1:S_2:W_2:S_3 = 89.5:20:1:40:49.5$ as a test case. This can be a difficult situation for the SDA program to obtain an accurately converged result for any modal solution. Due to the strong coupling between the adjacent edges, a sufficient number of bases and a sufficiently large number of spectral terms are required to obtain very accurate results. Similar experience was reported in [10], where a square matrix of order 20 and 10^5 spectral summation terms were used to obtain accurate electromagnetic field solutions for a narrow microstrip with a shielding/line width ratio of 30. Here, a square matrix order from 32 to 40 (16 to 20 for one strip) and a number of spectral terms N from 10^4 to 10^5 are used in the SDA program to perform the comparative convergence study of various types of bases.

The discretized, or subdomain, bases [13] are also incorporated into the SDA to verify the solutions. Each conducting strip is partitioned into M intervals of equal width, and the modeling of current distributions in each interval is similar to that of [13] except that the first three terms of (5) and (6) are used to account for the edge condition in the outermost intervals. These unconditioned subdomain bases enforced with the edge condition are simply called the unconditioned bases or the subdomain bases throughout the paper.

The results reported herein are obtained by using the RM/FORTRAN version 2.4 on an IBM personal computer or the VAX/VMS FORTRAN on a VAX-3200 workstation. Both result in the same answers for all the particular case studies presented here. Since one of the goals of this work is to obtain modal solutions that are as accurate as possible, faster converging algorithms, such as the technique reported in [7] are not used. No approximation is made except for the truncation on the finite number of spectral summation terms N. All the variables in the SDA program are declared as double precision to maintain the best accuracy.

A. Convergence Study of the Modal Solution of the Strongly Coupled Microstrip Lines

Table I presents the solution of the complex mode of the asymmetric strongly coupled microstrip lines analyzed at 150 GHz. Two aspects of the convergence study will be discussed, namely the number of spectral terms (N) and the number of basis functions (N_b). The bases adopted in Table I fall into two classes, namely preconditioned bases and unconditioned subdomain bases.

TABLE I
CONVERGENCE STUDY OF THE NORMALIZED PROPAGATION CONSTANT OF A COMPLEX MODE OF THE SUSPENDED ASYMMETRIC STRONGLY COUPLED MICROSTRIP LINES.

N		10^4	5×10^4
Bases	N_b*2	γ/k_0*3 $= \alpha/k_0 + j\beta/k_0$	$\gamma/k_0 = \alpha/k_0 + j\beta/k_0$
S type*1	6	1.5445488+j0.018984261	1.5445533+j0.018982025
	8	1.5445237+j0.019005269	1.5445285+j0.019003067
	10	1.5445128+j0.019012435	1.5445178+j0.019010247
C type*1	6	1.5457003+j0.019166921	1.5457056+j0.019164078
	8	1.5456979+j0.019167201	1.5457034+j0.019164305
	10	1.5456974+j0.019167248	1.5457030+j0.019164324
Proposed bases*1	3	1.5444925+j0.019006956	1.5444999+j0.019004243
	4	1.5444954+j0.019019870	1.5445019+j0.019017659
	5	1.5444955+j0.019019970	1.5445020+j0.019017690
Subdomain bases M*4	20	1.5445036+j0.019018027	1.5445099+j0.019015763
	40	1.5444991+j0.019019360	1.5445055+j0.019017006
N		10^5	
Subdomain bases M	20	1.5445107+j0.019015488	
	40	1.5445063+j0.019016728	

Structural parameters: $2a = 2.54$ mm, $S_1 = 1.13665$ mm, $W_1 = 0.254$ mm, $S_2 = 0.0127$ mm, $W_2 = 0.508$ mm, $S_3 = 0.62865$ mm, $h_1 = h_2 = 0.254$ mm, $h_3 = 0.762$ mm; $\epsilon_{r1} = \epsilon_{r3} = 1$, $\epsilon_{r2} = 2.2$; frequency = 150 GHz.

*1 These sets of bases belong to the class of preconditioned or entire-domain or global basis functions. The S and C type bases stand for sinusoidal [10], [11] and Chebyshev [12] types of bases, respectively.

*2 N_b is the number of the basis functions used to expand J_z or J_x on each conducting strip. The matrix size for the proposed set of bases is $8N_b \times 8N_b$, and for the S or C type of bases it is $4N_b \times 4N_b$.

*3 Normalized complex propagation constant, k_0 being the wavenumber in free space.

*4 M is the number of equally partitioned intervals of each conducting strip. The first three edge terms in (5) and (6) are incorporated into the subdomain bases for both J_z and J_x at the outermost intervals. The matrix size is $4(M+3)\times 4(M+3)$.

The results obtained by the SDA using the preconditioned S and C types and the proposed bases are compared. Then the nearly converged solutions obtained by these preconditioned bases will be compared with those obtained by the unconditioned subdomain bases.

To expand J_z and J_x on a conducting strip, the proposed set of bases uses a total of $4N_b$ basis terms, compared with the S or C type, which applies $2N_b$ terms. Therefore the matrix $\boldsymbol{G}$ in (3) established by the proposed bases for the asymmetric coupled microstrip lines is $8N_b \times 8N_b$ in size, and that established by the S or C type is $4N_b \times 4N_b$. For the same matrix size, we list the results with $N_b = 6$, 8, and 10 for the S and C types whereas $N_b = 3$, 4, and 5 for the proposed bases. The subdomain bases, however, need not have the same matrix size. Since we are interested in the nearly converged results, only the solutions with $M = 20$ and $M = 40$ are presented.

On the other hand, the results with $N = 10^4$ and 5×10^4 are presented for all types of bases, except that an additional case with $N = 10^5$ terms is used for the subdomain bases.

As shown in Table I, the normalized propagation constants, i.e. γ/k_0 $(=\alpha/k_0 + j\beta/k_0)$, converge to $6.9\times10^{-4}\%$ $(3.8\times10^{-2}\%)$, $2.6\times10^{-5}\%$ $(9.9\times10^{-5}\%)$, and $6.5\times10^{-6}\%$ $(1.6\times10^{-4}\%)$ for α (β) obtained by the use of S type, C type, and proposed bases, respectively, when the matrix size is increased from 32×32 to 40×40 with $N = 5\times10^4$. As N increased from 10^4 to 5×10^4 with matrix size 40×40, it is seen that all three preconditioned bases have resulted in approximately the same convergence rate with respect to N, i.e. $4\times10^{-4}\%$ $(10^{-2}\%)$ for α (β). Next we compare the apparently converged results obtained by the preconditioned bases, i.e., the solutions with $N = 5\times10^4$, $N_b = 10$ for the S or C type, and $N_b = 5$ for the proposed bases, with those obtained by the subdomain bases with $M = 40$ and $N = 10^5$. We find that the normalized propagation constant obtained by the subdomain bases agrees with those by the S type, C type, and proposed bases to $7.4\times10^{-4}\%$ $(3.4\times10^{-2}\%)$, $7.7\times10^{-2}\%$ $(7.8\times10^{-1}\%)$ and $2.8\times10^{-4}\%$ $(5.1\times10^{-3}\%)$ accuracy for α (β), respectively. Compared with bases of the S and C types the solutions obtained by the proposed bases have the closest agreement with those obtained by the unconditioned subdomain bases.

We do not know yet which set of basis functions results in the closest solution to the true current. Thus the next subsection plots the complex modal J_z and J_x current distributions for the comparative study.

B. Current Distributions on Strongly Coupled Microstrips: Capability of Modeling True Current Distributions — Criterion 5

The preconditioned basis functions in the SDA are required in order to represent the true modal current distributions. For the particular case of the asymmetric strongly coupled microstrip lines discussed in subsection III-A, the current distributions for the complex modes obtained by the proposed bases may nearly converge by using $N_b = 4$ and $N = 5\times10^4$, whereas bases of the S type and the C type require the use of $N_b = 10$ and $N = 5\times10^4$.

Parts (a) through (d) of Fig. 3 illustrate the magnitude and phase of the normalized J_z and J_x on strips 1 and 2 for one of the complex modes. All the current components are normalized by the total longitudinal current on strip 1, i.e., I_1. Using the same structural parameters and the same complex mode in Table I, the results obtained by the unconditioned subdomain bases and various preconditioned bases are presented. The number of spectral terms N and the number of intervals M used for the case of subdomain bases are 10^5 and 40, respectively.

As shown in parts (a) through (d) of Fig. 3, the normalized current distributions obtained by the S type and C type bases are oscillatory. Not shown in these figures is the fact that the magnitudes of the oscillations surrounding the plots computed on the basis of the proposed bases decrease as N_b increases from 6 to 10. The current distributions presented for the S and C type bases are those for $N_b = 10$. In an average sense, all the bases result in close agreement for the normalized J_{z1} and J_{z2} components; however, the normalized J_{x1} and J_{x2} obtained by bases of the C type deviate appreciably from those obtained by the others. Notice that the longitudinal (J_{z1} or J_{z2}) and transverse (J_{x1} or J_{x2}) currents of the complex mode are comparable in magnitude while the longitudinal

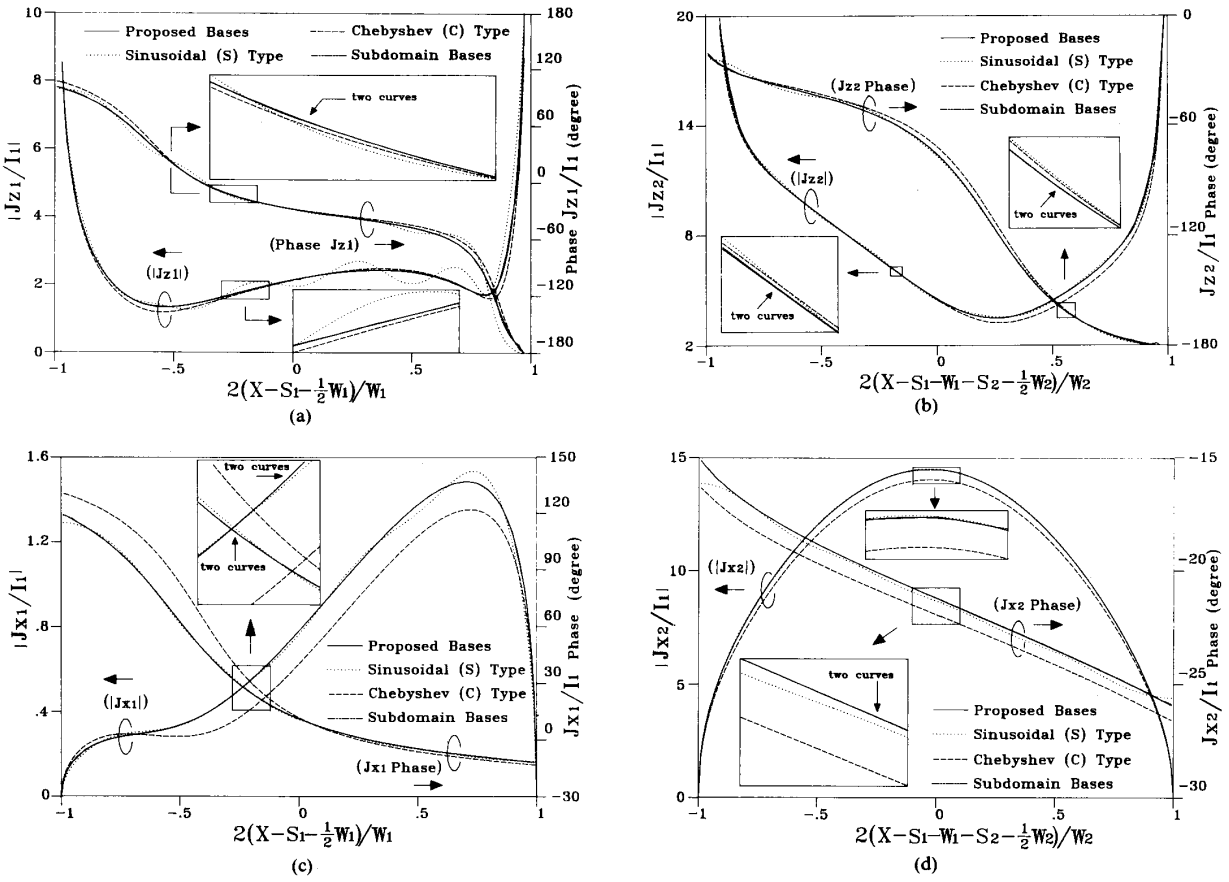

Fig. 3. Comparison of the complex mode current distributions obtained by the unconditioned subdomain and various types of preconditioned bases. The test conditions and the values of the normalized propagation constants for the complex modes are given in Table I. $N_b = 10$ and $N = 5 \times 10^4$ for both the S and C type bases; $N_b = 4$ and $N = 5 \times 10^4$ for the proposed bases; and $M = 40$ and $N = 10^5$ for the subdomain bases. (a) Magnitude and phase of the normalized J_z distribution on strip 1. (b) Magnitude and phase of the normalized J_z distribution on strip 2. (c) Magnitude and phase of the normalized J_x distribution on strip 1. (d) Magnitude and phase of the normalized J_x distribution on strip 2.

currents may be approximately two orders of magnitude bigger than the transverse currents for the dominant modes. This reflects the fact that the normalized complex propagation constants obtained by bases of the C type converge to slightly different real part (α) values than those obtained by other types of bases, as shown in Table I.

For the case of the proposed bases the current distributions are in excellent agreement with those obtained by the subdomain bases. This supports the fact that the normalized propagation constants obtained by subdomain bases are in closest agreement with those obtained by the proposed bases (See Table I).

For the dominant c and π modes under the same test conditions, i.e., the strongly coupled microstrip lines, the convergence of the propagation constant and the normalized current distributions obtained by the unconditioned and the three types of preconditioned basis functions has also been investigated. It was found that the above-mentioned results for the complex mode also apply to these two dominant modes. Thus the proposed set of bases is capable of modeling true currents on coupled microstrip lines.

C. Fundamental, Higher Order, Evanescent, and Complex Modes in Suspended Coupled Microstrip Lines

Some of the important features of the complex modes and the backward-wave modes of planar transmission lines were thoroughly discussed in [4]. Here, theoretical results for various types of modes of the suspended coupled microstrip lines are presented for the first time. For all the modal solutions shown later, the normalized propagation constant $\gamma/k_0(\alpha/k_0 + j\beta/k_0)$ is plotted against frequency. The evanescent modes are in the lower parts of the figures. For one of a pair of complex modes, the normalized phase constant β/k_0 and the normalized attenuation constant α/k_0 are represented by a dotted line and a dashed line, respectively. Since the convergence study of the modal solutions has been established in subsections III-A and III-B, the search of the modal

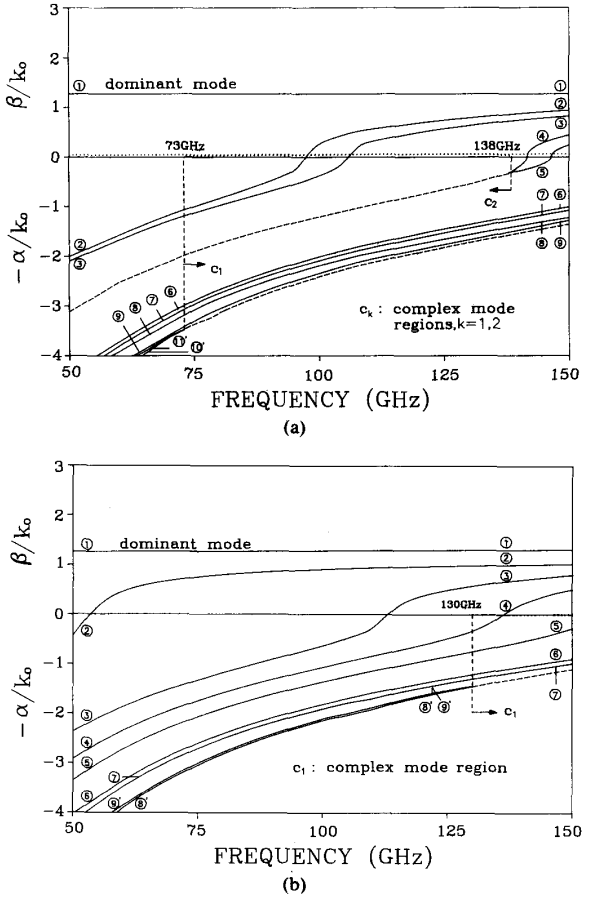

Fig. 4. Normalized propagation constant $\gamma/k_0 = \alpha/k_0 + j\beta/k_0$ of the suspended coupled microstrip lines versus frequency. Structural parameters: $2a = 2.54$ mm, $S_1 = S_3 = 1.1049$ mm, $W_1 = W_2 = 0.127$ mm, $S_2 = 0.0762$ mm, $3h_1 = h_2 = 0.381$ mm, $h_3 = 0.762$ mm; $\epsilon_{r1} = \epsilon_{r3} = 1$, $\epsilon_{r2} = 2.2$. (a) Odd-mode excitation. (b) Even-mode excitation.

solutions is carried out by using the proposed basis functions with $N_b = 3$.

Parts (a) and (b) of Fig. 4 plot the odd- and even-mode dispersion characteristics of the particular suspended coupled microstrip lines, respectively. At the high-frequency end, the dominant mode is designated as mode 1, the first higher order mode as mode 2, and so on. Reading from the right of each figure, the primed number denotes the mode coming out of the complex mode region. The backward-wave and complex mode regions are designated as b_k and c_k, respectively. The subscript k denotes different regions for the backward-wave and complex modes in the figure. The W-band (75–110 GHz) waveguide housing of 2.54×1.27 mm^2 (100×50 mil^2) is used. The relative dielectric constant of the suspended substrate is 2.2, and the thickness is 15 mils.

The odd-mode case of Fig. 4(a) consists of two distinct sets of complex modes. One ranges from under 50 GHz to 138 GHz, the other from 73 GHz to beyond 150 GHz. Notice that these two regions of complex modes have nearly the same values of imaginary (β) parts. In the case of the even mode, Fig. 4(b) indicates that the first higher order mode has a cutoff frequency near 55 GHz, which is the reduction of the cutoff frequency of an air-filled W-band waveguide (59 GHz) due to the presence of the dielectric layer. The first pair of complex modes is beyond 130 GHz.

Keeping the same physical structure as used in Fig. 4 except for an increase in the relative dielectric constant from 2.2 to 10, the odd-mode case of Fig. 5(a) has four sets of backward-wave modes and nine regions of complex modes, and the modal solutions become much more complicated than those in Fig. 4(a). Notice that mode 1 and mode 2, and mode 6 and mode 7 do not intersect as shown in the zoomed windows. Similarly, Fig. 5(b) of the even-mode case has at least two and six sets of backward-wave and complex modes, respectively, in the frequency spectrum plotted.

Through the particular case studies investigated, a few observations from the modal solutions with complex modes are made: 1) the complex modes and the backward-wave modes may start to appear as the second and the third higher order modes (See Fig. 5); 2) the complex modes may start to appear in the third and fourth higher order modes even when a low-dielectric-constant substrate is used (See Fig. 4(a)); 3) the complex modes may spread entirely beyond the frequency spectrum of interest for certain suspended coupled microstrip lines (See Fig. 4(a)); 4) the complex modes may repeatedly occur within a certain frequency band (See Fig. 5(a)); and 5) the above-cutoff higher order modes may result in the generation of complex modes (See Fig. 5(b)).

Therefore, for the particular case study of the suspended coupled microstrip lines, it is important to take into account the existence of the complex modes in formulating the discontinuity problem.

IV. Conclusion

An extensive convergence study of the full-wave spectral-domain analysis (SDA) of quasi-planar suspended coupled microstrip lines is presented. It validates the use of the proposed set of bases incorporated into the SDA program. In particular, the case of the suspended strongly coupled microstrip lines is investigated thoroughly. The comparative analyses of the normalized current distributions, which are obtained by the proposed bases and other commonly used preconditioned and unconditioned bases, indicate that the solutions based on the proposed bases exhibit the smoothest current distributions for the complex modes and have excellent agreement with those obtained by the unconditioned subdomain bases. Thus this paper provides a viable set of basis functions for the SDA in analyzing transmission lines of planar or quasi-planar structures.

Of more importance is the fact that the suspended coupled microstrip lines may have complex modes which start to appear as the first few higher order modes even when a substrate of low dielectric constant ($\epsilon_r = 2.2$) is

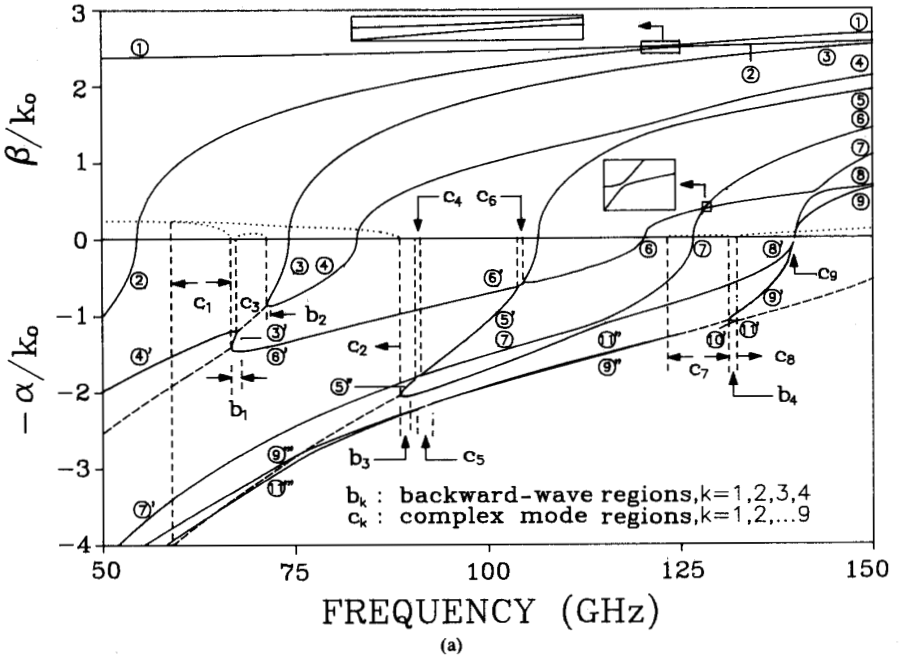

Fig. 5. Normalized propagation constant $\gamma/k_0 = \alpha/k_0 + j\beta/k_0$ of the suspended coupled microstrip lines versus frequency. Structural parameters: $2a = 2.54$ mm, $S_1 = S_3 = 1.1049$ mm, $W_1 = W_2 = 0.127$ mm, $S_2 = 0.0762$ mm, $3h_1 = h_2 = 0.381$ mm, $h_3 = 0.762$ mm; $\epsilon_{r1} = \epsilon_{r3} = 1$, $\epsilon_{r2} = 10$. (a) Odd-mode excitation. (b) Even-mode excitation.

used. In contrast to the suspended coupled microstrip lines, the symmetric finline may have complex modes at fairly higher order modes, say the eighth higher order mode [8]. Thus the characterization of the discontinuity problem of the suspended coupled microstrip lines would have inaccurate results if the effects of the complex modes were not included in the analysis. The results presented in this paper may prove useful for understanding the operation of microwave or millimeter-wave circuits integrated by suspended coupled microstrip lines involving discontinuities.

REFERENCES

[1] T. Itoh, "Overview of quasi-planar transmission lines," *IEEE Trans. Microwave Theory Tech.*, vol. 37, pp. 275–280, Feb. 1989.

[2] R. G. Arnold, I. G. Eddison, and R. H. Jansen, "A comprehensive CAD approach to the design of MMIC's up to millimeter-wave frequencies," *IEEE Trans. Microwave Theory Tech.*, vol. 36, pp. 208–219, Feb. 1988.

[3] N. H. L. Koster and R. H. Jansen, "The microstrip discontinuity: A revised description," *IEEE Trans. Microwave Theory Tech.*, vol. MTT-34, pp. 213–223, Feb. 1986.

[4] A. S. Omar and K. F. Schünemann, "Formulation of the singular integral equation technique for planar transmission lines," *IEEE Trans. Microwave Theory Tech.*, vol. MTT-33, pp. 1313–1322, Dec. 1985.

[5] A. S. Omar and K. F. Schünemann, "Complex and backward-wave modes in inhomogeneously and anisotropically filled waveguides," *IEEE Trans. Microwave Theory Tech.*, vol. MTT-35, pp. 268–275, Mar. 1987.

[6] W.-X. Huang and T. Itoh, "Complex modes in lossless shielded microstrip lines," *IEEE Trans. Microwave Theory Tech.*, vol. 36, pp. 163–165, Jan. 1988.

[7] C. J. Railton and T. Rozzi, "Complex modes in boxed microstrip," *IEEE Trans. Microwave Theory Tech.*, vol. 36, pp. 865–874, May 1988.

[8] A. S. Omar and K. F. Schünemann, "The effect of complex modes at finline discontinuities," *IEEE Trans. Microwave Theory Tech.*, vol. MTT-34, pp. 1508–1514, Dec. 1986.

[9] R. H. Jansen, "High-speed computation of single and coupled microstrip parameters including dispersion, higher order modes, loss and finite thickness," *IEEE Microwave Theory Tech.*, vol. MTT-26, pp. 75–82, Feb. 1978.

[10] R. H. Jansen, "Unified user-oriented computation of shielded, covered, and open planar microwave and millimeter-wave transmission line characteristics," *Microwave, Opt. Acoust.*, vol. 3, no. 1, pp. 14–22, Jan. 1979.

[11] L. P. Schmidt, T. Itoh, and H. Hofmann, "Characteristics of unilateral fin-line structures with arbitrarily located slots," *IEEE Trans. Microwave Theory Tech.*, vol. MTT-29, pp. 352–355, Apr. 1981.

[12] V. K. Tripathi and H. Lee, "Spectral-domain computation of characteristic impedances and multiple ports coupled microstrip lines," *IEEE Trans. Microwave Theory Tech.*, vol. 37, pp. 215–221, Jan. 1989.

[13] N. Faché and D. D. Zutter, "Rigorous full-wave space domain solution for dispersive microstrip lines," *IEEE Trans. Microwave Theory Tech.*, vol. 36, pp. 731–737, Apr. 1988.

[14] R. H. Jansen, "The spectral domain approach for microwave integrated circuits," *IEEE Trans. Microwave Theory Tech.*, vol. MTT-33, pp. 1043–1056, Oct. 1985.

[15] T. Itoh, "Spectral domain immitance approach for dispersion characteristics of generalized printed transmission lines," *IEEE Trans. Microwave Theory Tech.*, vol. MTT-28, pp. 733–736, July 1980.

[16] J. D. Jackson, *Classical Electrodynamics*. New York: Wiley, 1975, ch. 2.

[17] E. J. Denlinger, "A frequency dependent solution for microstrip transmission lines," *IEEE Trans. Microwave Theory Tech.*, vol. MTT-19, pp. 30–39, Jan. 1971.

[18] M. Abramowitz and I. A. Stegun, Eds., *Handbook of Mathematical Functions with Formulas, Graphs, and Mathematical Tables*. New York: Dover, 1964, p. 300.

[19] M. Kobayashi and F. Ando, "Dispersion characteristics of open microstrip lines," *IEEE Trans. Microwave Theory Tech.*, vol. MTT-35, pp. 101–105, Feb. 1987.

[20] M. Kobayashi and H. Momoi, "Longitudinal and transverse current distributions on coupled microstrip lines," *IEEE Trans. Microwave Theory Tech.*, vol. 36, pp. 588–593, Mar. 1988.

[21] N. Faché and D. D. Zutter, "Circuit parameters for single and coupled microstrip lines by a rigorous full-wave space-domain analysis," *IEEE Trans. Microwave Theory Tech.*, vol. 37, pp. 421–425, Feb. 1989.

✠

Jen-Tsai Kuo (S'89) received the B.S. degree in communication engineering from National Chiao Tung University (NCTU) in 1981 and the M.S. degree in electrical engineering from National Taiwan University in 1984, both in Taiwan, Republic of China. Since August 1984, he has been with the Department of Communication Engineering at NCTU, where he is working toward the Ph.D. degree and is a research assistant in the Microelectronics and Information Science and Technology Research Center. He is also a lecturer at the Microwave and Communication Electronics Laboratory. His research interests include microwave and millimeter-wave integrated circuit design.

✠

Ching-Kuang C. Tzuang (S'84–M'87) was born in Taiwan on May 10, 1955. He received the B.S. degree in electronic engineering from National Chiao Tung University, Hsinchu, Taiwan, in 1977 and the M.S. degree from the University of California at Los Angeles in 1980.

From February 1981 to June 1984, he was with TRW, Redondo Beach, CA, working on analog and digital monolithic microwave integrated circuits. He received the Ph.D. degree in electrical engineering in 1986 from the University of Texas at Austin, where he worked on high-speed transient analyses of monolithic microwave integrated circuits. Since September 1986, he has been with the Institute of Communication Engineering, National Chiao Tung University, Hsinchu, Taiwan, R.O.C. His research activities involve the design and development of millimeter-wave and microwave low-noise amplifiers, nonlinear oscillators, mixers, isolators, filters, and applied microwave field theory.